Published in final edited form as:
Cancer Res. 2013 July 15; 73(14): 4362–4371. doi:10.1158/0008-5472.CAN-12-3154.

Structure-specific endonucleases Xpf and Mus81 play overlapping but essential roles in DNA repair by homologous recombination

Koji Kikuchi[1,*], **Takeo Narita**[1,*], **Pham Thanh Van**[1], **Junko Iijima**[1], **Kouji Hirota**[1], **Islam Shamima Keka**[1], **Mohiuddin**[1], **Katsuya Okawa**[2], **Tetsuya Hori**[3], **Tatsuo Fukagawa**[3], **Jeroen Essers**[4,5], **Roland Kanaar**[5], **Matthew C. Whitby**[6], **Kaoru Sugasawa**[7], **Yoshihito Taniguchi**[1], **Katsumi Kitagawa**[8], and **Shunichi Takeda**[1,†]

[1]Department of Radiation Genetics, Graduate School of Medicine, Kyoto University, Yoshidakonoe, Sakyo-ku, Kyoto 606-8501, Japan [2]Frontier Technology Center, Graduate School of Medicine, Kyoto University, Yoshidakonoe, Sakyo-ku, Kyoto 606-8501, Japan [3]Department of Molecular Genetics, National Institute of Genetics and Sokendai, Mishima, Shizuoka 411-8540, Japan [4]Department of Vascular Surgery, Erasmus University Medical Center, PO Box 2040, 3000 CA, Rotterdam, The Netherlands [5]Department of Genetics and Department of Radiation Oncology, Cancer Genomics Center, Erasmus University Medical Center, PO Box 2040, 3000 CA, Rotterdam, The Netherlands [6]Department of Biochemistry, University of Oxford, South Parks Road, Oxford OX1 3QU, UK [7]Biosignal Research Center, Organization of Advanced Science and Technology, Kobe University, Hyogo 657-8501, Japan [8]Center for Childhood Cancer, The Research Institute at Nationwide Children's Hospital, 700 Children's Drive, Columbus, Ohio 43205, USA

Abstract

DNA double-strand breaks (DSBs) occur frequently during replication in sister chromatids, and are dramatically increased when cells are exposed to chemotherapeutic agents including camptothecin. Such DSBs are efficiently repaired specifically by homologous recombination (HR) with the intact sister chromatid. HR hence plays pivotal roles in cellular proliferation and cellular tolerance to camptothecin. Mammalian cells carry several structure-specific endonucleases, such as Xpf-Ercc1 and Mus81-Eme1, in which Xpf and Mus81 are the essential subunits for enzymatic activity. Here we show the functional overlap between Xpf and Mus81 by conditionally inactivating Xpf in the chicken DT40 cell line, which has no Mus81 ortholog. Although mammalian cells deficient in either Xpf or Mus81 are viable, Xpf inactivation in DT40 cells was lethal, resulting in a marked increase in the number of spontaneous chromosome breaks. Similarly, inactivation of both Xpf and Mus81 in human HeLa cells and murine embryonic stem cells caused numerous spontaneous chromosome breaks. Furthermore, the phenotype of Xpf-deficient DT40 cells was reversed by ectopic expression of human Mus81-Eme1 or human Xpf-Ercc1 heterodimers. These observations indicate the functional overlap of Xpf-Ercc1 and Mus81-Eme1 in the maintenance of genomic DNA. Both Mus81-Eme1 and Xpf-Ercc1 contribute to the completion of HR as evidenced by the following data that the expression of Mus81-Eme1 or Xpf-Ercc1 diminished the number of camptothecin-induced chromosome breaks in Xpf-deficient DT40 cells, and preventing early steps in HR by deleting *XRCC3* suppressed the inviability of Xpf-

[†]Correspondence: Department of Radiation Genetics, Graduate School of Medicine, Kyoto University, Yoshidakonoe, Sakyo-ku, Kyoto 606-8501, Japan; phone +81-75-753-4410l; fax +81-75-753-4419; stakeda@rg.med.kyoto-u.ac.jp.
[*]The first two authors contributed equally to this work.

Conflict of interest: No conflict of interest exists.

deficient DT40 cells. In summary, Xpf and Mus81 have a substantially overlapping function in completion of HR.

Keywords

homologous recombination; Xpf; Mus81; nuclease; chemotherapeutic agents

Introduction

Homologous recombination (HR) mediated double-strand break (DSB) repair is initiated by resection of DSBs and formation of 3′ single-strand overhangs, followed by polymerization of Rad51 (1, 2). The resulting nucleoprotein filaments, consisting of the 3′ single-strand tail and the polymerized Rad51, undergo homology search and pairing with the intact duplex DNA donor to form a displacement (D)-loop structure. Extensive strand exchange of the D-loop leads to the generation of HR intermediates. HR intermediates are processed into either crossover products or non-crossover products (3). HR intermediates including Holliday junction (HJ) are hereafter called joint molecules (JMs).

The processing of JMs is carried out by dissolution and resolution pathways. In the dissolution pathway, Sgs1 (Blm, an ortholog of Sgs1 in human), topoisomerase III, and RMI1/2 collaboratively catalyze the decatenation of HJs and generate non-crossover products (4-6). In the resolution pathway, structure-specific endonucleases cleave the HJs and produce crossover and non-crossover products, depending on the choice of cleaved strands at the four-way junction (7). In *E. coli*, the RusA nuclease and the RuvABC complex cleave HJs symmetrically and play a key role in the resolution pathway (8-10). Recent work with eukaryotes has revealed two resolvases, Gen1 (11) and the Slx1-Slx4 complex (12-15), both of which can symmetrically cleave the four-way junction. A third enzyme called Mus81 together with its partner Eme1/Mms4 has also been implicated in resolving HJs and the formation of crossover recombinants in both mitotic and meiotic recombination in yeast and mammals (16, 17). *In vitro* data show an ability of Mus81 to incise HJs asymmetrically, however a greater predilection for cleaving D-loops and nicked HJs suggests that unlike “classical” HJ resolvases Mus81 may process JMs before they mature into fully ligated HJs (16).

Mus81 is a member of the Xpf family of structure-specific endonucleases. Human Xpf is best known for its role in nucleotide excision repair (NER), together with its partner Ercc1. Moreover, Xpf, but not the other NER factors, is involved in DSB repair including single-strand annealing (18, 19), incision at interstrand crosslinks (20), and gene targeting (21). However, no studies have reported a functional overlap between Mus81 and Xpf in any DNA repair or recombination reactions, or a role of Xpf in HR after the formation of JMs. Intriguingly the Xpf orthologs in both Drosophila and *C. elegans* have been implicated in JM processing and the formation of crossovers during meiosis. Whether Xpf is similarly involved in JM processing in vertebrates alongside enzymes like Mus81 is currently unknown.

To investigate the role of Xpf in HR, we conditionally disrupted the *XPF* gene in the chicken B lymphocyte line DT40 (22). Because this line does not possess the *MUS81* gene, we propose that the loss of Xpf in DT40 cells is equivalent to mammalian cells deficient in both Xpf and Mus81. Deletion of *XPF* caused extensive chromosomal aberrations and cell death. However, this lethality was substantially reversed by ectopic expression of human Mus81 together with Eme1 (HsMus81-Eme1), indicating a compensatory relationship between Xpf and Mus81 in the maintenance of chromosomal DNA. The phenotypic analysis

of Xpf-depleted DT40 cells indicated that a marked genomic instability may result from the defective processing of JMs. Our data uncovered that the Xpf and Mus81 endonucleases play overlapping and essential roles in completion of HR.

Materials and Methods

Cell culture, plasmid constructs, and siRNAs

Chicken DT40, mouse embryonic stem (ES) (*wild-type* (IB10) and *MUS81*$^{-/-}$), and HeLa cells were cultured as described previously (23-25). DT40 or ES cells have been maintained by S. Takeda or J. Essers since 1991 or 2004, respectively (22, 24). HeLa cells were obtained from K. Myung (NHGRI) in 2007 (25). All of cell lines were tested routinely for various criteria such as morphology, growth rate, and karyotype. Details for plasmid constructs, and siRNAs are provided in SI materials and methods.

Cell cycle analysis

After BrdU pulse-labeling in the cells exposed to tamoxifen (TAM), cell-cycle distribution was measured as described previously (26).

Measurement of chromosomal aberrations

Chromosomal aberrations were measured as described previously (23). Briefly, the cells were exposed to TAM for 1, 2, or 3 days, with 0.1 μg/ml of colcemid added for the last 3 h of incubation before harvest. To measure IR-induced chromosomal aberrations, the cells were exposed to TAM for 24 h, and colcemid was added immediately after cells were irradiated with 0.3 Gy γ-rays. To test the response to CPT, cells were continuously exposed to TAM for 33 h, with the cells treated with 100 nM CPT for the last 9 h, and also treated with colcemid for the last 3 h before harvest of mitotic cells.

Measurement of Rad51 subnuclear foci

Before measurement of Rad51 subnuclear foci, cells were exposed to TAM for 2 days. Rad51 foci were visualized with anti-Rad51 antibody in untreated cells and in cells γ-irradiated with 4 Gy, 3 h and 6 h after treatment as previously described (26).

Measurement of SCE levels

SCE levels were measured as described previously (27). Before BrdU labeling, cells were exposed to TAM for 30 h. Cells were cultured in the presence of 10 μM BrdU for 21 h and treated with 0.1 μg/ml of colcemid for the last 3 h. CPT (5 nM or 100 nM) was added 9 h before harvest.

Measurement of chromosome aberrations in HeLa and mouse ES cells

Chromosomal aberrations were measured as described previously (23). Briefly, transfection of siRNA into HeLa or mouse ES cells using lipofectamine RNAiMAX or lipofectamine 2000 was performed according to the manufacturer's instructions, respectively. 45 h after the transfection, HeLa cells were incubated for 1 h with 0.2 μg/ml colcemid after which metaphase cells were collected by mitotic shake-off. Alternatively, 72 h after the transfection, mouse ES cells were incubated for 2 h with 0.1 μg/ml colcemid after which metaphase cells were collected by mitotic shake-off.

Statistics

We did three independent experiments for all of data sets. The results were expressed as mean ± SD (growth curves and sensitivity to the genotoxic agents) or mean ± SEM

(chromosomal aberrations and SCEs). Differences between the data were tested for statistical significance using t-test.

Additional details are provided in SI materials and methods.

Results

Mus81 protein is absent in chicken DT40 cells

Chicken *XPF* cDNA encodes a putative 903 amino-acid proteins, compared to the 905 amino-acids of human Xpf (Supplementary Fig. S1). The sequence identity between the two proteins is 76.8%. As expected, immunoprecipitants of tagged Xpf included Ercc1 (Supplementary Fig. S2A and B), indicating that Xpf associates with Ercc1 in DT40 cells. Since there is an ortholog of Eme1 but not Mus81 registered in the chicken genome database (Supplementary Fig. S3A and B) (28), we analyzed proteins that interact with Eme1, which forms a heterodimer with Mus81 in mammalian cells. Immunoprecipitants of tagged Eme1 included Xpf, but not Mus81 (Supplementary Fig. S4A), indicating the absence of functional Mus81-Eme1 complex in DT40 cells. To verify the absence of Mus81-Eme1, we disrupted the *EME1* gene (Supplementary Fig. S5A). $EME1^{-/-}$ DT40 cells were able to proliferate and showed moderate sensitivity only to cisplatin (Supplementary Fig. S5B and C), which phenotype is in marked contrast with the hypersensitivity of mouse $EME1^{-/-}$ and $MUS81^{-/-}$ ES cells to a wide variety of DNA damaging agents (29, 30). We therefore concluded no Mus81 ortholog in DT40 cells.

The data indicate that the relationship among Xpf, Mus81, Eme1 and Ercc1 differs between DT40 and mammalian cells. The moderate sensitivity of $EME1^{-/-}$ DT40 cells to cisplatin (Supplementary Fig. S5C) indicates that Xpf might form a functional complex with Eme1, whereas mammalian Mus81 and Xpf form a heterodimer with Eme1 and Ercc1, respectively. This idea is supported by the data that, consistent with a previous report (31), interaction of Xpf with Eme1 was confirmed by co-immunoprecipitation of recombinant proteins (Supplementary Fig. S4B and C). In addition to the presence of Xpf-Eme1, it should be noted that we could not formally exclude the possibility that a functional homolog of Mus81 is present in chicken cells. In conclusion, Xpf-Ercc1, but not Xpf-Eme1, plays the major role in DNA damage response in chicken cells.

Deletion of *XPF* results in an accumulation of chromosomal aberrations and subsequent cell death

We generated *XPF* gene-disruption constructs, which deleted amino-acid coding sequences 1 to 148 together with the transcriptional promoter sequences (Fig. 1A and supplementary Fig. S6A). Because we failed to establish $XPF^{-/-}$ cells from $XPF^{+/-}$ cells, we generated conditional Xpf-deficient cells using a chicken *XPF* transgene flanked by loxP-signal sequences (*GdXPF-loxP*), which is excised by the chimeric Cre recombinase carrying the TAM-binding domain (Supplementary Fig. S6B). Since the *GdXPF-loxP* transgene also carries a marker gene encoding the Green Fluorescent Protein (GFP), TAM-mediated excision of the *GdXPF-loxP* transgene can be evaluated by monitoring the loss of the GFP signal (Supplementary Fig. S6C and D). We also confirmed depletion level of *XPF* mRNA by RT-PCR (Supplementary Fig. 6E). We generated $XPF^{+/-}$ *GdXPF-loxP* clones, and subsequently generated two $XPF^{-/-}$ *GdXPF-loxP* clones, which displayed indistinguishable phenotypes.

We analyzed the proliferation kinetics of the cells with and without treatment with TAM (Fig. 1B and C). The $XPF^{+/+}$, $XPF^{+/-}$ *GdXPF-loxP* and $XPF^{-/-}$ *GdXPF-loxP* cells without the TAM treatment divided every 8 h (Supplementary Fig. S6F). By contrast, at ~2 day after treatment with TAM, the $XPF^{-/-}$ cells ceased to proliferate (Fig. 1B and C). To explore the

cause of this mortality, we examined spontaneously arising chromosomal aberrations in mitotic cells. It should be noted that chromosomal breaks hereafter represent discontinuities, which appear on chromosomes in metaphase spreads as regions unstained by Giemsa, and do not always result from DSBs. We found a dramatic increase in the number of chromosomal aberrations prior to cell death in the Xpf-deficient cells (Fig. 1D), an occurrence that is consistently observed in cells that have a severe defect in HR (26, 32-34), but is not observed in DT40 cells deficient in the *XPA* or *XPG* genes involved in NER (35, 36). To test whether the nuclease activity of Xpf is required for cellular viability, we created two cDNAs mutated at the catalytic center of Xpf, Gd*XPF*(D674A) and Gd*XPF*(D702A) (Supplementary Figs. S1 and S6G). In contrast to a *wild-type* Xpf transgene, these mutant transgenes yielded no stable clones (Supplementary Fig. S6G), suggesting that the mutant Xpf proteins may interfere with the endogenous Xpf by competing for the association with Ercc1.

HR-mediated DSB repair is severely compromised in Xpf-deficient cells

To analyze the role of Xpf in HR, we assessed the capability of HR-mediated DSB repair at 24 h after TAM treatment, when the cells were still able to proliferate exponentially. To selectively evaluate HR-mediated DSB repair, we measured the number of chromosomal aberrations in mitotic cells following exposure of cells to camptothecin (CPT), a DNA topoisomerase I poison, and to γ-rays in the G_2 phase. CPT induces single-end breaks during replication, and the restart of replication requires HR with the intact sister chromatid (37). Similarly, γ-ray-induced chromosomal aberrations are repaired exclusively by HR in the G_2 phase in DT40 cells (38).

Xpf-depleted cells had a greater number of CPT-induced chromosomal aberrations than did Xpf-expressing cells (Fig. 2A). We next exposed an asynchronous population of cells to γ-rays and measured the number of chromosomal aberrations in cells that entered the M phase within 3 h after irradiation. This protocol allows for the evaluation of DSB repair selectively during the G_2 phase, where HR plays a dominant role in DSB repair (38). Following irradiation, the total number of chromosomal aberrations in Xpf-deficient cells increased to 0.26 per cell, whereas the total number in $XPF^{+/+}$ cells increased only to 0.08 (Fig. 2B). Taken together, these results indicate that Xpf plays a key role in HR-mediated DSB repair.

HR-mediated DSB repair in *XPF* mutant cells is compromised at a late step

To differentiate between the early and late steps of HR, we analyzed the formation of γ-ray-induced Rad51 foci (Fig. 2C). At 3 h after IR, there was no change in the rate of Rad51 focus formation for Xpf-expressing or Xpf-depleted cells. However, the Rad51 foci continued to be formed by 6 h in Xpf-depleted cells, whereas the foci were decreased in Xpf-expressing cells. This suggests that Xpf is required for the completion of HR after formation of the Rad51 nucleofilament. To assess the role of Xpf in the late steps of HR, i.e., during JM formation and processing, we measured the number of SCEs, which represent crossover-type HR (27). The number of CPT-induced SCEs in Xpf-depleted cells was only 40% of the number in Xpf-expressing cells (Fig. 2D), indicating that Xpf is required for crossover-type HR.

If the mortality of the $XPF^{-/-}$ cells is caused by impaired completion of HR, it might be reversed by blocking the initiation of HR. To test this hypothesis, we disrupted the *XRCC3* gene in $XPF^{-/-}$*GdXPF-loxP* cells. Xrcc3 facilitates an initial step of HR by promoting the polymerization of Rad51 at DNA lesions (39). To generate $XPF^{-/-}/XRCC3^{-/-}$ cells, we exposed the resulting $XPF^{-/-}$*GdXPF-loxP*/$XRCC3^{-/-}$ cells to TAM. This mutant displayed lower levels of cell death (Fig. 3A) and a significant decrease in the number of chromosomal aberrations (Fig. 3B), compared to Xpf-depleted cells, though the $XRCC3^{-/-}$ cells did

display moderate genomic instability (23, 39). These observations support the conclusion that Xpf plays a critical role in the completion of HR-mediated repair after the polymerization of Rad51 at DNA lesions.

We next considered that if Xpf contributes to HR after the formation of JMs, the severe phenotype of Xpf-depleted cells might be suppressed by ectopic expression of *E. coli* RusA resolvase (40). To generate *XPF*$^{-/-}$ cells stably expressing RusA, *XPF*$^{-/-}$*GdXPF-loxP* cells were transfected with RusA cDNA, and the resulting *XPF*$^{-/-}$*GdXPF-loxP/RusA* cells were exposed to TAM. The RusA expression improved cellular viability (Fig. 3C) and decreased the number of spontaneous chromosomal aberrations in Xpf-depleted cells (Fig. 3D). Intriguingly, the reduction in chromosome-type breaks is associated with an increase in chromatid-type breaks. Similarly RusA expression resulted in a decrease in γ-ray-induced chromosome-type breaks without affecting the number of chromatid-type breaks (Fig. 3E). These data are consistent with the idea that chromosome-type breaks result from a failure to complete HR after the formation of JMs in Xpf-deficient cells.

Human Mus81-Eme1 and Xpf-Ercc1 contribute to HR by processing joint molecules

The absence of both Xpf and Mus81 in *XPF*$^{-/-}$ DT40 cells provides us with the novel opportunity of investigating the role of human Xpf-Ercc1 and Mus81-Eme1 in HR. To generate *XPF*$^{-/-}$*/HsXPF-ERCC1* and *XPF*$^{-/-}$*/HsMUS81-EME1* cells, *XPF*$^{-/-}$*GdXPF-loxP* cells were transfected with HsXpf-Ercc1 or HsMus81-Eme1 cDNA, and *XPF*$^{-/-}$*GdXPF-loxP* cells stably expressing HsXpf-Ercc1 or HsMus81-Eme1 were exposed to TAM. Note that we failed to generate *XPF*$^{-/-}$*/HsMUS81* cells probably due to instability of HsMus81 as a consequence of poor association with GdEme1. HsXpf-Ercc1 reversed the mortality in *XPF*$^{-/-}$ DT40 cells (Fig. 4A). Remarkably, HsMus81-Eme1 also significantly restored the cellular proliferation of *XPF*$^{-/-}$ DT40 cells to a level comparable to the cells complemented with HsXpf-Ercc1 (Fig. 4C), though the amino acid sequence identity between GdXpf and HsMus81 is only 9.7%. Next we analyzed *XPF*$^{-/-}$*/HsXPF-ERCC1* and *XPF*$^{-/-}$*/HsMUS81-EME1* cells by counting both spontaneous (Fig. 4B and D) and γ-ray-induced chromosomal aberrations (Fig. 5A and B). In all cases, the ectopic expression of the human enzymes suppressed the chromosomal aberrations caused by Xpf deficiency and particularly chromosome-type breaks. These observations indicate that HsMus81-Eme1 and HsXpf-Ercc1 have very similar functions in HR-mediated DNA repair and genome maintenance.

To determine whether HsMus81-Eme1 promotes crossover-type HR, we counted the number of SCEs in *XPF*$^{-/-}$*/HsMUS81-EME1* cells. The expression of HsMus81-Eme1 restored the number of CPT-induced SCEs (Fig. 5C) to the number of SCEs in GdXpf-expressing cells (Fig. 2D). We conclude that Mus81 and Xpf have very similar functions in promoting crossover-type HR.

Finally, we tested whether Xpf and Mus81 compensate for each other in the completion of HR in human and mouse cell lines. We depleted Xpf and Mus81 in human HeLa cells or depleted Xpf in mouse *MUS81*$^{-/-}$ ES cells, using small interfering RNA (siRNA) (Supplementary Fig. S7A and B). In HeLa cells, the depletion of both Xpf and Mus81, but not the depletion of either Xpf or Mus81 alone, increased the number of spontaneous chromosome-type breaks (Fig. 6A). Similarly, depletion of Xpf in mouse *MUS81*$^{-/-}$ embryonic stem (ES) cells greatly increased the number of spontaneous chromosome-type breaks, compared with Xpf-depleted *wild-type* and mock-transfected *MUS81*$^{-/-}$ ES cells, while they showed only a moderate increase in the number of spontaneous chromosome-type breaks (Fig. 6B). These results indicate that the role of Xpf in HR is conserved in mammalian and DT40 cells.

Discussion

We have shown that the Xpf and Mus81 structure-specific endonucleases compensate for each other in the maintenance of chromosomal DNA. This compensatory relationship is verified by the following phenotypic analysis of Xpf-deficient DT40 cells, which lack a *MUS81* ortholog. First, the expression of HsMus81-Eme1 as well as HsXpf-Ercc1 reversed the mortality of Xpf-deficient DT40 cells (Figs. 4 and 5). Second, the mortality of Xpf-deficient DT40 cells is in marked contrast to the viability of Xpf-deficient mammalian cells (41, 42) and to the normal development of Mus81-deficient mice (24, 43). Third, although chicken Xpf and Eme1 physically interact with each other (Supplementary Fig. S4B and C), GdXpf-Eme1 has a minor role in genome maintenance (Supplementary Fig. S5), and does not account for mortality of Xpf-deficient DT40 cells. Finally, our findings using DT40 cells are applicable to mammals as evidenced by the fact that inactivation of both Xpf and Mus81 caused increased the number of chromosome-type breaks in human HeLa and mouse ES cells (Fig. 6). These observations demonstrate that the two structure-specific endonucleases have substantially overlapping functions in the maintenance of genomic DNA.

We have provided a few different lines of evidence that collectively indicate that Xpf contributes to HR-dependent DSB repair probably after the formation of JMs made of broken sister chromatids and the other intact ones. First, the inactivation of Xpf resulted in prolonged Rad51 foci formation (Fig. 2C). Second, the expression of Xpf and Mus81 enhanced the formation of SCEs (Fig. 2D and 5C). Third, preventing the initiation of HR by deleting *XRCC3* suppressed the mutant phenotype of Xpf-deficient DT40 cells (Fig. 3A and B). These results indicated that Xpf plays a role in HR at a late step. Conceivably, the inactivation of Xpf may cause a defect in the separation of JMs prior to mitosis, which defect is more toxic than the defective formation of JMs due to the absence of *XRCC3*.

The loss of viability in Xpf-deficient DT40 cells is associated with chromosome aberrations, which appear on metaphase spreads as regions unstained by Giemsa. Throughout we have referred to these as chomatid-type breaks and chromosome-type breaks depending on whether the discontinuity in staining affects one or both sister chromatids, respectively. In the case of chromatid-type breaks, we suspect that the absence of Giemsa staining actually represents a DSB in the sister chromatid as these aberrations are also observed in mutants that are defective for early steps of HR (44). However, we think that the chromosome-type breaks represent regions of uncondensed DNA rather than actual broken chromosomes similar to what was recently reported (45). It is proposed that regions devoid of Giemsa staining occur at sites of sister chromatid entanglement, which inhibits chromosome condensation. Importantly the chromosome-type breaks that we observe in Xpf-deficient cells both spontaneously and following γ-ray exposure are suppressed by ectopic expression of the HJ resolvase RusA (Fig. 3D and E) providing strong evidence that they result from unprocessed JMs. The fact that ectopic expression of HsXpf-Ercc1 and HsMus81-Eme1 also suppress chromosome-type breaks in Xpf-deficient DT40 cells suggests that there is a significant overlap in function between these enzymes that is most likely related to processing JMs such as D-loops and nicked single HJs.

Cells deficient in Xpf-Ercc1 are considerably more sensitive to chemical crosslinking agents than cells deficient in the other NER factors, indicating the critical role for Xpf-Ercc1 in interstrand crosslink (ICL) repair. Although there is compelling evidence that the critical role played by Xpf is carried out by introducing single-strand breaks at cross-links to initiate ICL repair (20, 46), Xpf may function in ICL repair also by facilitating HR. We recently found that Slx4 links the FA-dependent ICL pathway with both Mus81 and Xpf, as Slx4 serves as docking sites for the two nucleases and the ubiquitinated FancD2 protein, which finding agrees with recent reports showing FA patients carrying mutations in the *SLX4* gene

(47-49). Taking into account the fact that Slx4 also binds to the Slx1 5′-flap endonucleaseand in addition to the Mus81-Eme1 and Xpf-Ercc1 3′-flap endonucleases (Supplementary Fig. S2A and S4D) (12-15), these endonucleases may collaboratively work in ICL repair by promoting the completion of HR. In this scenario, it is not surprising that the two 3′-flap endonucleases are complementary to each other. Future studies will analyze the interdependent and complementary relationships of multiple endonucleases when they carry out a variety of DNA repair reactions.

Supplementary Material

Refer to Web version on PubMed Central for supplementary material.

Acknowledgments

We thank R. Ohta and Y. Satoh for their technical assistance. We also thank Dr. M. Lisby for sharing unpublished data.

Grant Support Financial support was provided in part by a grant-in-aid from the Ministry of Education, Culture, Sports, Science and Technology of the Japanese Government (MEXT) (grant number 20241012 to S.T. and grant number 22700881 to K.K.), a grant from The Kanae Foundation (to K.K.), grants from the European Community's Seventh Framework Programme (FP7/2007-2013) under grant agreement No. HEALTH-F2-2010-259893 and from the Netherlands Genomics Initiative / Netherlands Organization for Scientific Research (to R.K.), and NIH grants GM68418 and CA133093 (to K.Kitagawa).

References

1. Takeda S, Nakamura K, Taniguchi Y, Paull TT. Ctp1/CtIP and the MRN complex collaborate in the initial steps of homologous recombination. Mol. Cell. 2007; 28:351–2. [PubMed: 17996697]
2. Bernstein KA, Rothstein R. At loose ends: resecting a double-strand break. Cell. 2009; 137:807–10. [PubMed: 19490890]
3. Bzymek M, Thayer NH, Oh SD, Kleckner N, Hunter N. Double Holliday junctions are intermediates of DNA break repair. Nature. 2010; 464:937–41. [PubMed: 20348905]
4. Wu LaH ID. The Bloom's syndrome helicase suppresses crossing over during homologous recombination. Nature. 2003; 426:870–4. [PubMed: 14685245]
5. Xu D, Guo R, Sobeck A, Bachrati CZ, Yang J, Enomoto T, Brown GW, Hoatlin ME, Hickson ID, Wang W. RMI, a new OB-fold complex essential for Bloom syndrome protein to maintain genome stability. Genes Dev. 2008; 22:2843–55. [PubMed: 18923082]
6. Chu WK, Hickson ID. RecQ helicases: multifunctional genome caretakers. Nat. Rev. Cancer. 2009; 9:644–54. [PubMed: 19657341]
7. Schwartz E, Heyer WD. Processing of joint molecule intermediates by structure-selective endonucleases during homologous recombination in eukaryotes. Chromosoma. 2011; 120(2):109–27. [PubMed: 21369956]
8. Macmaster R, Sedelnikova S, Baker PJ, Bolt EL, Lloyd RG, Rafferty JB. RusA Holliday junction resolvase: DNA complex structure—insights into selectivity and specificity. Nucleic Acids Res. 2006; 34:5577–84. [PubMed: 17028102]
9. Shinagawa H, Iwasaki H. Processing the holliday junction in homologous recombination. Trends Biochem. Sci. 1996; 21:107–11. [PubMed: 8882584]
10. West SC. Processing of recombination intermediates by the RuvABC proteins. Annu. Rev. Genet. . 1997; 31:213–44. [PubMed: 9442895]
11. Ip SC, Rass U, Blanco MG, Flynn HR, Skehel JM, West SC. Identification of Holliday junction resolvases from humans and yeast. Nature. 2008; 456:357–61. [PubMed: 19020614]
12. Andersen SL, Bergstralh DT, Kohl KP, LaRocque JR, Moore CB, Sekelsky J. Drosophila MUS312 and the vertebrate ortholog BTBD12 interact with DNA structure-specific endonucleases in DNA repair and recombination. Mol. Cell. 2009; 35:128–35. [PubMed: 19595722]

13. Fekairi S, Scaglione S, Chahwan C, Taylor ER, Tissier A, Coulon S, Dong MQ, Ruse C, Yates JR 3rd, Russell P, Fuchs RP, McGowan CH, Gaillard PH. Human SLX4 is a Holliday junction resolvase subunit that binds multiple DNA repair/recombination endonucleases. Cell. 2009; 138:78–89. [PubMed: 19596236]
14. Munoz IM, Hain K, Declais AC, Gardiner M, Toh GW, Sanchez-Pulido L, Heuckmann JM, Toth R, Macartney T, Eppink B, Kanaar R, Chris P, Ponting CP, David MJ, Lilley DM, Rouse J. Coordination of structure-specific nucleases by human SLX4/BTBD12 is required for DNA repair. Mol. Cell. 2009; 35:116–27. [PubMed: 19595721]
15. Svendsen JM, Smogorzewska A, Sowa ME, O'Connell BC, Gygi SP, Elledge SJ, Harper JW. Mammalian BTBD12/SLX4 assembles a Holliday junction resolvase and is required for DNA repair. Cell. 2009; 138:63–77. [PubMed: 19596235]
16. Osman F, Dixon J, Doe CL, Whitby MC. Generating crossovers by resolution of nicked Holliday junctions: a role for Mus81-Eme1 in meiosis. Mol Cell. 2003; 12(3):761–74. [PubMed: 14527420]
17. Holloway JK, Booth J, Edelmann W, McGowan CH, Cohen PE. MUS81 generates a subset of MLH1-MLH3-independent crossovers in mammalian meiosis. PLoS Genet. 2008; 4(9):e1000186. [PubMed: 18787696]
18. Niedernhofer LJ, Odijk H, Budzowska M, van Drunen E, Alex Maas A, Theil AF, de Wit J, Jaspers NG, Beverloo B, Hoeijmakers JH, Kanaar R. The structure-specific endonuclease Ercc1-Xpf is required to resolve DNA interstrand cross-link-induced double-strand breaks. Mol. Cell. Biol. 2004; 24:5776–87. [PubMed: 15199134]
19. Pâques, FaH; J.E.. Multiple pathways of recombination induced by double-strand breaks in *Saccharomyces cerevisiae*. Microbiol. Mol. Biol. Rev. 1999; 63:349–404. [PubMed: 10357855]
20. Knipscheer P, Räschle M, Smogorzewska A, Enoiu M, Ho TV, Schärer OD, Elledge SJ, Walter JC. The Fanconi anemia pathway promotes replication-dependent DNA interstrand cross-link repair. Science. 2009; 326(5960):1698–701. [PubMed: 19965384]
21. Niedernhofer LJ, Essers J, Weeda G, Beverloo B, de Wit J, Muijtjens M, Odijk H, Hoeijmakers JH, Kanaar R. The structure-specific endonuclease Ercc1-Xpf is required for targeted gene replacement in embryonic stem cells. EMBO J. 2001; 20:6540–9. [PubMed: 11707424]
22. Buerstedde, JMaT; S. Increased ratio of targeted to random integration after transfection of chicken B cell lines. Cell. 1991; 67:179–88. [PubMed: 1913816]
23. Fujimori A, Tachiiri S, Sonoda E, Thompson LH, Dhar PK, Hiraoka M, Takeda S, Zhang Y, Reth M, Takata M. Rad52 partially substitutes for the Rad51 paralog XRCC3 in maintaining chromosomal integrity in vertebrate cells. EMBO J. 2001; 20:5513–20. [PubMed: 11574483]
24. McPherson JP, Lemmers B, Chahwan R, Pamidi A, Migon E, Matysiak-Zablocki E, Moynahan ME, Essers J, Hanada K, Poonepalli A, Sanchez-Sweatman O, Khokha R, Kanaar R, Jasin M, Hande MP, Hakem R. Involvement of mammalian Mus81 in genome integrity and tumor suppression. Science. 2004; 304:1822–6. [PubMed: 15205536]
25. Motegi A, Sood R, Moinova H, Markowitz SD, Liu PP, Myung K. Human SHPRH suppresses genomic instability through proliferating cell nuclear antigen polyubiquitination. J. Cell Biol. 2006; 175(5):703–8. [PubMed: 17130289]
26. Yamaguchi-Iwai Y, Sonoda E, Sasaki MS, Morrison C, Haraguchi T, Hiraoka Y, Yamashita YM, Yagi T, Takata M, Price C, Kakazu N, Takeda S. Mre11 is essential for the maintenance of chromosomal DNA in vertebrate cells. EMBO J. 1999; 18:6619–29. [PubMed: 10581236]
27. Sonoda E, Sasaki MS, Morrison C, Yamaguchi-Iwai Y, Takata M, Takeda S. Sister chromatid exchanges are mediated by homologous recombination in vertebrate cells. Mol. Cell. Biol. 1999; 19:5166–9. [PubMed: 10373565]
28. http://genome.ucsc.edu/cgi-bin/hgBlat
29. Abraham J, Lemmers B, Hande M,P, Moynahan ME, Chahwan C, Ciccia A, Essers J, Hanada K, Chahwan R, Khaw AK, McPherson P, Shehabeldin A, Laister R, Arrowsmith C, Kanaar R, West SC, Jasin M, Hakem R. Eme1 is involved in DNA damage processing and maintenance of genomic stability in mammalian cells. EMBO J. 2003; 22:6137–47. [PubMed: 14609959]
30. Hanada K, Budzowska M, Modesti M, Maas A, Wyman C, Essers J, Kanaar R. The structure-specific endonuclease Mus81-Eme1 promotes conversion of interstrand DNA crosslinks into double-strands breaks. EMBO J. 2006; 25:4921–32. [PubMed: 17036055]

31. Ciccia A, Ling C, Coulthard R, Yan Z, Xue Y, Meetei AR, et al. Identification of FAAP24, a Fanconi anemia core complex protein that interacts with FANCM. Mol Cell. 2007; 25(3):331–43. [PubMed: 17289582]
32. Sonoda E, Sasaki MS, Buerstedde JM, Bezzubova O, Shinohara A, Ogawa H, Takata M, Yamaguchi-Iwai Y, Takeda S. Rad51-deficient vertebrate cells accumulate chromosomal breaks prior to cell death. EMBO J. 1998; 17:598–608. [PubMed: 9430650]
33. Nakahara M, Sonoda E, Nojima K, Sale JE, Takenaka K, Kikuchi K, Taniguchi Y, Nakamura K, Sumitomo Y, Bree RT, Lowndes NF, Takeda S. Genetic evidence for single-strand lesions initiating Nbs1-dependent homologous recombination in diversification of Ig v in chicken B lymphocytes. PLoS Genet. 2009; 5:e1000356. [PubMed: 19180185]
34. Nakamura K, Kogame T, Oshiumi H, Shinohara A, Sumitomo Y, Agama K, Pommier Y, Tsutsui KM, Tsutsui K, Hartsuiker E, Ogi T, Takeda S, Taniguchi Y. Collaborative action of Brca1 and CtIP in elimination of covalent modifications from double-strand breaks to facilitate subsequent break repair. PLoS Genet. 2010; 6:e1000828. [PubMed: 20107609]
35. Okada T, Sonoda E, Yamashita YM, Koyoshi S, Tateishi S, Yamaizumi M, Takata M, Ogawa O, Takeda S. Involvement of vertebrate polkappa in Rad18-independent postreplication repair of UV damage. J. Biol. Chem. 2002; 277:48690–5. [PubMed: 12356753]
36. Kikuchi K, Taniguchi Y, Hatanaka A, Sonoda E, Hochegger H, Adachi N, Matsuzaki Y, Koyama H, van Gent DC, Jasin M, Takeda S. Fen-1 facilitates homologous recombination by removing divergent sequences at DNA break ends. Mol. Cell. Biol. 2005; 25:6948–55. [PubMed: 16055708]
37. Pommier Y, Leo E, Zhang H, Marchand C. DNA topoisomerases and their poisoning by anticancer and antibacterial drugs. Chem. Biol. 2010; 17:421–33. [PubMed: 20534341]
38. Sonoda E, Hochegger H, Saberi A, Taniguchi Y, Takeda S. Differential usage of non-homologous end-joining and homologous recombination in double strand break repair. DNA Repair. 2006; 5:1021–9. [PubMed: 16807135]
39. Takata M, Sasaki MS, Tachiiri S, Fukushima T, Sonoda E, Schild D, Thompson LH, Takeda S. Chromosome instability and defective recombinational repair in knockout mutants of the five Rad51 paralog. Mol. Cell. Biol. 2001; 21:2858–66. [PubMed: 11283264]
40. Blais V, Gao H, Elwell CA, Boddy MN, Gaillard PH, Russell P, McGowan CH. RNA interference inhibition of Mus81 reduces mitotic recombination in human cells. Mol. Biol. Cell. 2004; 15(2): 552–62. [PubMed: 14617801]
41. Brookman KW, Lamerdin JE, Thelen MP, Hwang M, Reardon JT, Sancar A, Zhou ZQ, Walter CA, Parris CN, Thompson LH. ERCC4 (XPF) encodes a human nucleotide excision repair protein with eukaryotic recombination homologs. Mol. Cell. Biol. 1996; 16:6553–62. [PubMed: 8887684]
42. Tian M, Shinkura R, Shinkura N, Alt FW. Growth retardation, early death, and DNA repair defects in mice deficient for the nucleotide excision repair enzyme XPF. Mol. Cell. Biol. 2004; 24:1200–5. [PubMed: 14729965]
43. Dendouga N, Gao H, Moechars D, Janicot M, Vialard J, McGowan CH. Disruption of Murine Mus81 Increases Genomic Instability and DNA Damage Sensitivity but Does Not Promote Tumorigenesis. Mol. Cell. Biol. 2005; 25:7569–79. [PubMed: 16107704]
44. Sonoda E, Okada T, Zhao GY, Tateishi S, Araki K, Yamaizumi M, Yagi T, Verkaik NS, van Gent DC, Takata M, Takeda S. Multiple roles of Rev3, the catalytic subunit of polzeta in maintaining genome stability in vertebrates. EMBO J. 2003; 22:3188–97. [PubMed: 12805232]
45. Wechsler T, Newman S, West SC. Aberrant chromosome morphology in human cells defective for Holliday junction resolution. Nature. 2011; 471(7340):642–6. [PubMed: 21399624]
46. Wang AT, Sengerová B, Cattell E, Inagawa T, Hartley JM, Kiakos K, Burgess-Brown NA, Swift LP, Enzlin JH, Schofield CJ, Gileadi O, Hartley JA, McHugh PJ. Human SNM1A and XPF-ERCC1 collaborate to initiate DNA interstrand cross-link repair. Genes Dev. 2011; 25(17):1859–70. [PubMed: 21896658]
47. Crossan GP, van der Weyden L, Rosado IV, Langevin F, Gaillard PH, McIntyre R.E.; Sanger Mouse Genetics Project, Gallagher, F. Kettunen MI, Lewis DY, Brindle K, Arends MJ, Adams DJ, Patel KJ. Disruption of mouse Slx4, a regulator of structure-specific nucleases, phenocopies Fanconi anemia. Nat. Genet. 2011 doi:10.1038/ng.752.

48. Kim Y, Lach FP, Desetty R, Hanenberg H, Auerbach AD, Smogorzewska A. Mutations of the SLX4 gene in Fanconi anemia. Nat. Genet. 2011 doi:10.1038/ng.750.

49. Stoepker C, Hain K, Schuster B, Hilhorst-Hofstee Y, Rooimans MA, Steltenpool J, Oostra AB, Eirich K, Korthof ET, Nieuwint AW, Jaspers NG, Bettecken T, Joenje H, Schindler D, Rouse J, de Winter JP. SLX4, a coordinator of structure-specific endonucleases, is mutated in a new Fanconi anemia subtype. Nat. Genet. 2011 doi:10.1038/ng.751.

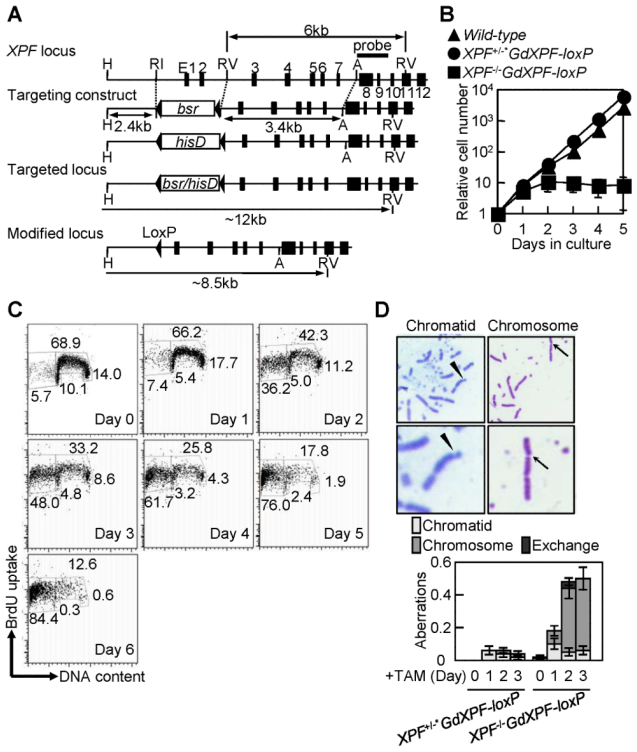

Figure 1. Xpf is essential for the maintenance of genome stability

(A) Targeted disruption of the chicken *XPF* gene. The chicken *XPF* locus, the two targeting constructs and the resulting targeted locus are shown. The black boxes represent the exons of the *XPF* gene. The triangles flanking the blastidine-resistance (bsr^R) and histidinol-resistance ($hisD^R$) genes represent the loxP sequences, the recognition site of the Cre recombinase. (B) Growth curve after addition of tamoxifen (TAM) to $XPF^{-/-}$ *GdXPF-loxP* cells at time zero for the excision of the *GdXPF-loxP* transgene. (C) Flow-cytometric analysis of cell-cycle distribution after BrdU pulse-labeling in $XPF^{-/-}$ *GdXPF-loxP* cells. (D) Spontaneous chromosomal aberrations in $XPF^{-/-}$ *GdXPF-loxP* cells. Top panels, a representative chromatid-type break (shown by arrowhead) and a chromosome-type break (shown by arrow). Breaks are magnified in the lower panels. Bottom panels, measurement of spontaneous chromosomal aberrations. A chromatid-type break indicates a discontinuity in one of the two sister chromatids, and a chromosome-type break indicates discontinuities at the same site of both sisters. Exchange indicates chromosomal translocation. The vertical axis shows the number of aberrations per cell.

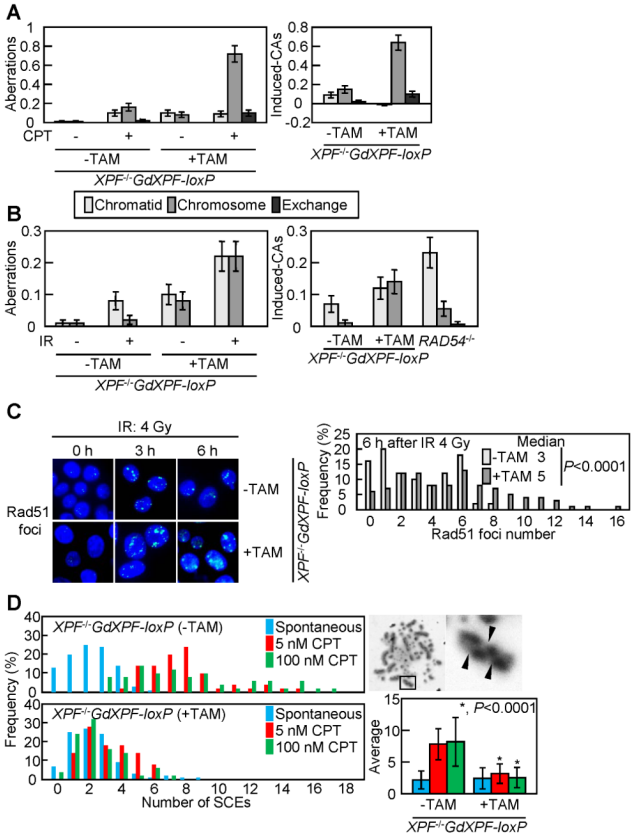

Figure 2. A defect in homologous-recombination-dependent DSB repair in Xpf-depleted cells

(A) Camptothecin (CPT)-induced chromosomal aberrations in Xpf-depleted cells. *XPF*$^{-/-}$ *GdXPF-loxP* cells were continuously exposed to TAM for 33 h, during which the cells were treated with 100 nM CPT for the last 9 h, and with colcemid for the last 3 h before harvest of mitotic cells. Left panels, measurement of chromosomal aberrations after treatment with or without CPT. Right panels, CPT-induced chromosomal aberrations were calculated by subtracting the number of spontaneously occurring chromosomal aberrations from the number of chromosomal aberrations observed in the CPT-treated sample of the same genotype. 100 mitotic cells were examined for each analysis. The vertical axis shows the number of aberrations per cell in A and B. (B) Ionizing radiation (IR)-induced chromosomal aberrations in Xpf-depleted cells. Cells were exposed to TAM for 24 h, exposed to γ-rays, then treated with colcemid for 3 h. Left panels, measurement of chromosomal aberrations after exposure to γ-rays. Right panels, IR-induced chromosomal aberrations were calculated by subtracting the number of spontaneously occurring chromosomal aberrations from the number of chromosomal aberrations observed in the γ-rays-exposed sample of the same genotype. Results of IR-induced chromosomal aberrations in *RAD54*$^{-/-}$ cells were described in a previous report (26). (C) The formation of γ-induced Rad51 foci in Xpf-expressing and Xpf-depleted cells. Left panels, a fraction of the γ-irradiation-induced Rad51 subnuclear foci persists for extended periods. Cells were exposed to TAM for 2 days, irradiated with 4 Gy γ-ray, fixed at 3 and 6 h post-IR, and subjected to immuno-cytochemistry using anti-Rad51 antibody. Right panels, quantification of Rad51 foci number at 6 h post-IR. 100 cells were examined for each analysis. (D) Xpf depletion reduces sister-chromatid exchange (SCE) events induced by CPT. The distribution of SCE events per cell is shown for the indicated cell samples to the left panels. Blue bars represent no CPT treatment, and red and green bars represent data for 5 nM and 100 nM CPT

treatment, respectively. Mean values and photo of a representative SCE (shown by arrowhead) are shown to the right panels.

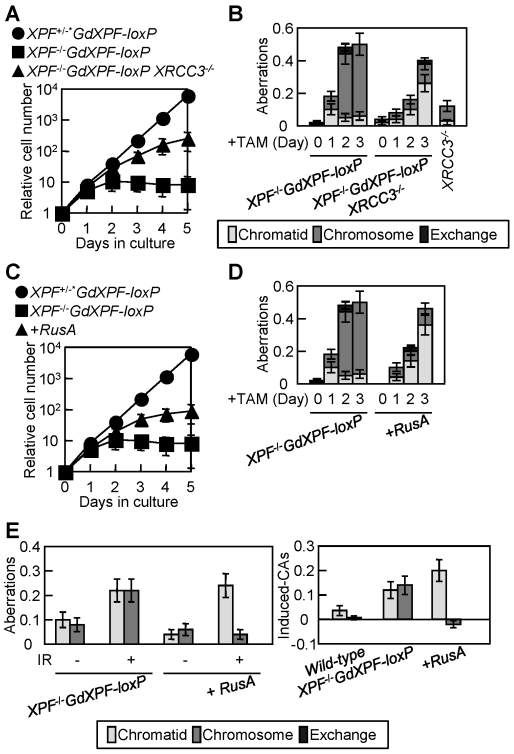

Figure 3. Deletion of the *XRCC3* reverses the mutant phenotype of *XPF*$^{-/-}$ cells

(A) Growth curve after adding TAM to *XPF*$^{-/-}$*GdXPF-loxP/XRCC3*$^{-/-}$ cells at time zero to inactivate the *GdXPF-loxP* transgene. (B) Spontaneous chromosomal aberrations in *XPF*$^{-/-}$*GdXPF-loxP/XRCC3*$^{-/-}$ cells were measured as described in Figure 1D. Results of spontaneous chromosomal aberrations for *XRCC3*$^{-/-}$ cells were described in a previous report (23). (C) Growth curve after adding TAM to the indicated cells at time zero. +RusA represents *XPF*$^{-/-}$*GdXPF-loxP* cells expressing RusA. (D) Spontaneous chromosomal aberrations in the indicated cells were measured as described in Figure 1D. (E) IR-induced chromosomal aberrations in *XPF*$^{-/-}$*/RusA* cells at 1 day after addition of TAM. Chromosomal aberrations induced by γ-rays were measured and calculated as described in Figure 2B.

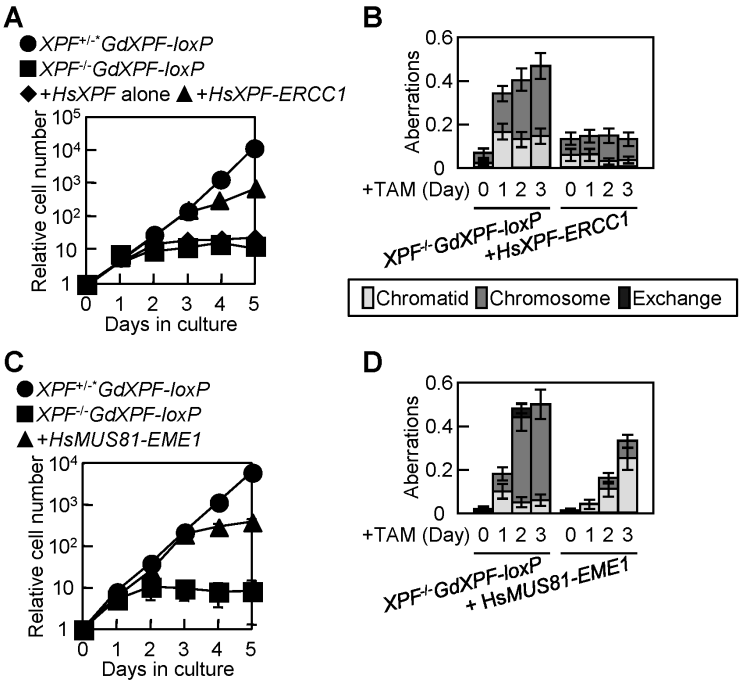

Figure 4. Ectopic expression of HsXpf-Ercc1 or HsMus81-Eme1 suppresses the lethality in *XPF*$^{-/-}$ cells

(A) Growth curve after addition of TAM to the indicated cells at time zero. + *HsXPF* alone and +*HsXPF-ERCC1* represent *XPF*$^{-/-}$ *GdXPF-loxP* cells expressing HsXpf alone and *XPF*$^{-/-}$ *GdXPF-loxP* cells expressing HsXpf-Ercc1, respectively. (B) Spontaneous chromosomal aberrations in the indicated cells were measured as described in Figure 1D. (C) Growth curve after addition of TAM to the indicated cells at time zero. +*HsMUS81-EME1* represents *XPF*$^{-/-}$ *GdXPF-loxP* cells expressing HsMus81-Eme1. (D) Spontaneous chromosomal aberrations in the indicated cells were measured as described in Figure 1D.

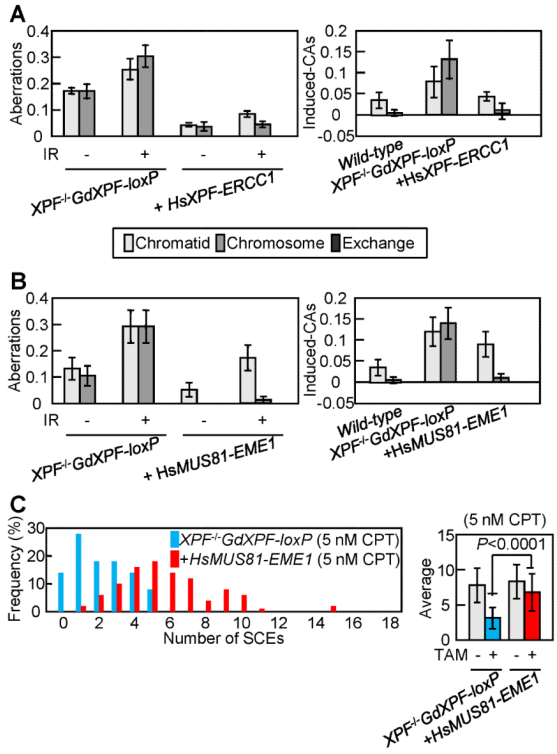

Figure 5. Ectopic expression of H HsXpf-Ercc1 or HsMus81-Eme1 reverses the mutant phenotype of *XPF*$^{-/-}$ cells

(A) IR-induced chromosomal aberrations in *XPF*$^{-/-}$*/HsXPF-ERCC1* cells at 1 day after addition of TAM. Chromosomal aberrations induced by γ-rays were measured and calculated as described in Figure 2B. (B) IR-induced chromosomal aberrations in *XPF*$^{-/-}$*/HsMUS81-EME1* cells at 1 day after addition of TAM. Chromosomal aberrations induced by γ-rays were measured and calculated as described in Figure 2B. (C) CPT-induced SCE events at 2 days after addition of TAM. The histograms to the left display the distribution of SCEs per cell following treatment with 5 nM CPT. Blue and red bars represent *XPF*$^{-/-}$ and *XPF*$^{-/-}$*/HsMUS81-EME1* cells, respectively. Mean values are shown to the right panels.

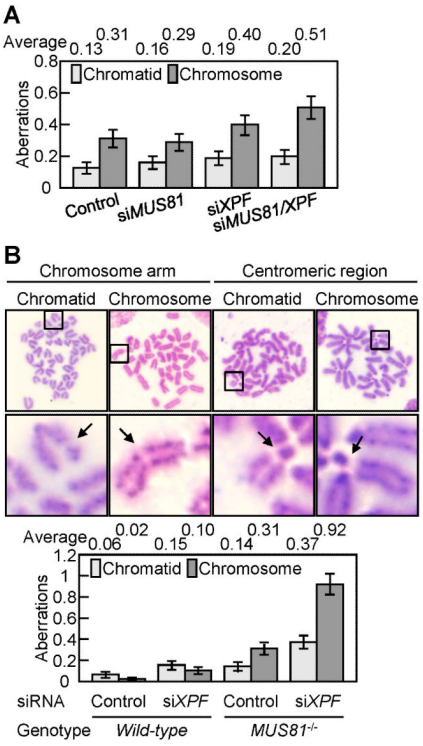

Figure 6. Xpf and Mus81 compensate for each other in the completion of HR in human and mouse cell lines

(A) After treatment with the indicated siRNAs in human HeLa cells, aberrant chromosomes in metaphase cells (n=200) were analyzed. The vertical axis shows the number of aberrations per cell in A and B.(B) After treatment with the indicated siRNAs in mouse wild-type or *MUS81*$^{-/-}$ cells, aberrant chromosomes in metaphase cells (n=100) were analyzed. A representative chromatid-type break and a chromosome-type break are magnified in the middle panels and are shown by arrow.